Stable Helicene Radicals: Synthesis, Structure, Physical Properties, and Photocatalysis

Aslam Shaikh
Department of Chemistry and Biochemistry, University of Arizona, Tucson, AZ, United States.
https://orcid.org/0000-0001-8818-2344
Md Mubarak Hossain
Department of Chemistry and Biochemistry, University of Arizona, Tucson, AZ, United States.
Jules Moutet
Department of Chemistry and Biochemistry, University of Arizona, Tucson, AZ, United States.
Jose Veleta
Department of Chemistry and Biochemistry, University of Arizona, Tucson, AZ, United States.
Jan Bloch
Department of Chemistry and Applied Biosciences, ETH Zürich, Zürich, Switzerland.
Andrei Astashkin
Department of Chemistry and Biochemistry, University of Arizona, Tucson, AZ, United States.
Thomas Gianetti (tgianetti@arizona.edu)
Department of Chemistry and Biochemistry, University of Arizona, Tucson, AZ, United States.
https://orcid.org/0000-0002-3892-3893

Article

Keywords: Stable [4]helicene radical, organic radical, Density functional calculations, EPR spectroscopy, X-ray crystallography, Photocatalysis, Photocatalytic dehalogenation

Posted Date: June 24th, 2020

DOI: https://doi.org/10.21203/rs.3.rs-36324/v1

Abstract

Stable organic radicals have gained considerable attention in the fields of catalysis and material sciences. In particular, helical molecules are of great interest in the development and application of novel organic radicals in optoelectronic and spintronic materials. Here we report the syntheses of highly stable neutral quinolinoacridine radicals by chemical reduction of their quinolinoacridinium cation analogs. The crystal structures of these [4]helicene radicals were determined by X-ray diffraction. Electron paramagnetic resonance (EPR) measurements, supported by density functional theory (DFT) calculations, indicate that the unpaired electron is mostly localized, showing more than 40% of spin density located at the central carbon of the [4]helicene radicals. Quantitative conversion from neutral radical to cation is observed upon exposure to air, monitored via UV-vis spectroscopy. The successful photoreductive dehalogenation of aryl halides occurs in the presence of 10 mol% of [4]helicene radical under blue light.

Introduction

Since the discovery of triphenylmethyl (trityl) radical by Gomberg in 1900,[1] many fundamental studies of persistent and stable carbon-based radicals have provided insight into their electronic structure, stability, and reactivity, such as hydrogen abstraction, dimerization, recombination and polymerization.[2][3][4][5][6] Yet the quest for new stable and isolable organic radicals is still ongoing. [7] Stable radicals are of particular interest to the scientific community for their potential applications in catalysis,[8][9][10] organic light-emitting diodes (OLEDs)[11][12][13] and other materials applications.[14][15][16][17] In recent years, organic radicals have received increasing interest due to their involvement in the fast growing field of photocatalysis.[18][19] During photoinduced electron transfer (PET) processess, an electron transfer occurs between the excited state of an organic photocatalyst (PC) and an electrochemically matching substrate, resulting in the formation of an organic radical.[20] The stability and electronic properties of the PC radical significantly influence the catalysis. Yet, in most systems, the radical moiety remains an unisolable transient intermediate. Interestingly, König in 2014[21] and Nicewicz in 2020[22] reported that organic radicals formed *in situ* as a result of PET from their closed- shell photocatalysts counterpart (perylenediimine PDI and mesityl acridnium salt Mes-Acr+, respectively) can further absorb light and efficiently catalyze the photoreduction of aryl halides. Despite early reports showing that transient organic radicals such as diarylketyl and diphenylmethyl can undergo PET,[23][24] PDI-• and Mes-Acr• are the only organic radical photocatalyst reported to date.

We recently reported the use of [4]helical carbeniums as efficient photocatalysts using a red LED as the energy source, generating [4]helicene radicals *in situ.*[25] To date, only a few examples of [*n*]helicene radicals (*n* = 4, 5, 6, 7 indicates the number of fused aromatic rings) have been reported in the literature.[26][27][28][29] The unpaired electron in these systems is stabilized through delocalization over the π-conjugated substituents, and the molecules with a higher number of fused aromatic rings show a higher stability. Thus, [4]helicenes represent the least stable and least studied radicals of this class. To the best of our knowledge, only four examples of [4]helicene radicals have been reported.[30][31][32][33] Of these

radicals, two showed limited stability,[30][31] and one was never isolated.[32] Notably, no X-ray crystallographic structure of any [4]helicene-based neutral radical has been reported.

Herein, we document the isolation, single crystal structure, and full characterization of a family of [4]-helicene radicals, namely, dimethoxyquinacridines (DMQA•), by 1H NMR, continuous wave (CW) EPR, electron-nuclear double resonance (ENDOR), cyclic voltammetry, UV–Vis absorption spectroscopy, and density functional theory (DFT) calculations. Furthermore, we report the reductive dehalogenation of aryl halides, including a relatively unreactive aryl chloride, under photocatalytic conditions using an isolated organic radical that possesses an excited state oxidation potential of - 2.9 V vs saturated calomel electrode (SCE).

Results And Discussion

Synthesis. The precursor [4]helicenium cations (*2+–5+)* were synthesized by adapting literature protocols (see Figure 1a and the Supporting Information (SI)),[34] and their formation was confirmed by 1H and 13C NMR spectroscopy (see SI) and X-ray crystallography (*vide infra).*. Unlike the carbocations *2-H*$^{+}$ and *3*$^{+}$*–5*$^{+,}$ the ^{1}H NMR spectrum of *2-NO2+* shows broad and poorly resolved resonances at room temperature, suggesting a dynamic exchange. Variable temperature (VT) 1H NMR spectroscopy analysis of *2-NO2+* over a temperature range of 193–333 K (Figure S13-S14) is consistent with the presence of an equilibrium between two conformers (Figure 1b). At 193 K, six methylenic protons are observed (Figure S15), three of which are diastereotopic according to a low-temperature 1H–1H COSY NMR sequence (Figure S17). These data suggest that *2-NO2+* favors a conformation containing an intramolecular NMe2–C^{+} interaction (Figure 1b).

Radicals *2•–5•* were obtained by reduction of *2+–5+,* respectively, with potassium metal in THF at room temperature overnight (Figure 1a and SI). The reaction mixture turned from a dark green suspension to a dark magenta solution. After filtration of the insoluble KBF4 salt formed and removal of THF under vacuum, the resultant solids were extracted with toluene. Crystallization from a toluene/hexane mixture at –35 °C afforded *2•–5•* as dark brown crystals in good yields (Figure 1a). The formation of radicals *2•–5•* was confirmed by EPR spectroscopy (*vide infra).*. Remarkably, the radicals formed are stable under inert atmosphere at room temperature in both the solid and solution over several months (See SI). The molecules *2•–5•* were analyzed by paramagnetic 1H NMR spectroscopy (Figure S22-S23). The protons of the substituent arms of the helicene consistently produce broad lines at 17 and –7 ppm, while the aromatic protons of the helicene radical scaffold are not observable. This suggests that the unpaired electron is delocalized across the fused heterocyclic rings and that the nature of the pendant arms has little influence on the radical character of *2•–5•.*

X-ray diffraction. Slow DCM/hexane layering afforded crystals of the cationic precursors 2-H+ and 2-NO2+ suitable for X-ray diffraction (XRD) analysis (Figure 1c). In both structures, the steric clash between the MeO groups results in a significant twist between the o-(MeO)-phenyl moieties (2-H+: 41.93°, 2-NO2+: 38.37°, see Table S5). The difference in torsion angles between 2-H+ and 2-NO2+ is also underlined by

the O1-O2 distances, 2.743 Å and 2.659 Å, respectively. As deduced from the VT 1H NMR results, one of the -nPr-NMe2 arms in 2-NO2+ is folded over the carbocation center with a C1- N3 distance of 3.194 Å, suggesting an increased Lewis acidity of the carbocation center conferred by the presence of the m-(NO2) group (Figure 1c and Table S5).

The neutral radicals *2-H*˙ and *2-NO2•* were isolated from a concentrated toluene solution by slow diffusion of hexane and analyzed by XRD (Figure 1c). The distortion of the *o-(*(MeO)-phenyl groups is more accentuated than for the cationic precursors in *2-H*˙ 45.92°, +3.99°), and particularly in *2-NO2•* *(*52.05°, +13.68°), resulting in similar O1-O2 distances for both molecules (*2-H*˙*:* 2.772 Å and *2-NO2• :* 2.773 Å) (Table S5). The increased C1-C2, C1-C3, and C1-C4 interatomic distances in *2-H•* *(*1.439(2), 1.444(3), and 1.446(3) Å, respectively) relative to the cation *2-H+ (*1.406(2), 1.435(2) and 1.431(2) Å) indicate an antibonding interaction between C1 and its surrounding atoms. Similarly, the C1-C3 bond in *2-NO2• (*1.429(3) Å) was elongated when compared to *2-NO2+ (*1.413(1) Å). In contrast, other bond distances around the central carbon (C1) in *2-NO2•* compared to those in *2-NO2+* were shortened (C1- C2 = 1.422(3) *vs* 1.431(1) Å) and unaffected (C1-C4 = 1.438(3) *vs* 1.440(1) Å), suggesting a structural or electronic effect of the NO2 group.

DFT calculations and EPR / ENDOR Measurements. The electronic structure of radicals *2•–5•* was studied using DFT calculations (See SI). Natural bond order (NBO) analyses revealed a considerable spin population (about 40%) localized on the central carbon (C1) in all radicals (Figure 2a and S24). This was observed regardless of the nature of the alkyl groups on the amino substituent or the presence of the electron withdrawing group NO2. A significant change, however, was observed in comparing the relative energies of the SOMOs (Figure S25), where the SOMOs of *2-NO2*˙ *(*––5.0 eV) appeared significantly stabilized by the electron withdrawing nitro group compared to *2-H*˙ *(*––4.4 eV).

EPR measurements were conducted in toluene solutions at room temperature to futher probe the electronic structure of these radicals (Figure 2b and SI). A Gaussian line centered at $g \approx 2.003$, with the width of about 0.76 mT was observed, with a poorly resolved hyperfine structure with a splitting of 0.088 mT for *2-H*˙ and *3*˙⁻*5*˙ trace 1 in Figure 2b(i)), and unresolved structure for *2-NO2• (*trace 2 in Figure 2a(i)). To gain insight into the hyperfine structure and the effect of the NO2 group, the ^{1}H ENDOR spectra were recorded (Figure 2b(ii) and SI). Radicals *2-H•* and *3•–5•* show three pairs of lines ((*a,a')*„ (*b,b')*„ and (*c,c')* (see trace 1 in Figure 2b(ii)), while *2-NO2•* presents a ~ 30% decrease of the relative intensity of (*b,b')* lines, and appearance of (*d,d')* and (*e,e')* lines (see trace 2 in Figure 2b(ii)). As shown by the X- ray studies, for *2-NO2•,* the substitution of a H by the NO2 group results in a significant conformational distortion of the aromatic ring structure and a reorientation of the CH2 group in the vicinity of NO2 (*vide supra).*. Since the DFT calculation for *2-NO2•* results in essentially the same distribution of spin populations as in *2-H•* and *3•–5•,* we tentatively assign these additional hfi constants to the protons of the reoriented CH2 group (Figure S29).

UV-Vis spectroscopy and Electrochemistry. The UV–visible spectra of the cations and radicals (*2–5)* were studied to futher probe the electronic structures of these molecules (Figure 3a). The blue shifted

absorptions of the radicals compared to their cation analogs (Figure 3a (i) and (ii)) indicate a reduced involvement of the heteroatoms in the molecular framework and a reduced conjugation across the π-system,[32] consistent with the increased distortion observed in solid state (*vide supra).*. The stability of *2•–5•* toward molecular oxygen was monitored upon exposure of their solution to air (*2-H•* Figure 3b) and *2-NO2•, 3•⁻5•* Figure S47, S49, S51, S53). Unlike most organic radicals, these DMQA radicals do not undergo oxygen insertion or dimer formation. Instead, a clean reversible oxidation to DMQA+ is observed. The radicals *2-H•* and *3•⁻5•* showed a significantly faster oxidation with t1/2 of 26–54 min compared to *2-NO2•* with t1/2 of 210 min (Figure S42). The reduced reactivity of *2-NO2•* is assigned to the inductive effect of the electron withdrawing NO2 groups (*vide supra* SOMO energy).[35][36][37][38]

To further understand the reacitivity difference of these [4]-helicene radicals, the electrochemical behavior of *2+–5+* was investigated by cyclic voltammetry (see Figure 3c and see SI for details). Under reductive conditions, a reversible event corresponding to the reduction of DMQA+ to DMQA• is observed around E1/2 = −1.25 V in 2^{+}–5^{+}.[32] This event is observed at a higher potential for *2-NO2+ (*−1.05 V), consistent with a more electron deficient scaffold and a reduced reactivity toward oxygen due to the presence of the NO2 group. A second redox event corresponding to the reduction of DMQA• to $DMQA^{-}$ was also present.[32] This was observed as a reversible process at E1/2 = −1.85 V for *2-NO2+,* and irreversible for $2\text{-}H^{+}$, 3^{+}–5^{+}, at E1/2 = −2.3 V.[32]

Photocatalysis. The estimated excited state oxidation potential of *2-H•* $E1/2(C^{+}/C^{\bullet *})$ = −2.79 V vs SCE, See SI) suggests a highly photoreducing species. The photocatalytic ability of *2-H•* was emphasized by the successful photo-reductive dehalogenation of aryl halides (X = I, Br, and Cl) under blue (Figure 4a) or green (Table S10) LED light. Aryl iodides were converted with high yield, while less reactive bromides and chlorides were reduced with good to moderate yields. A preliminary mechanistic study using 4-iodoaniline (*6b)* revealed that: i) absence of DIPEA led to no product formation (Table S9), ii) using Hantzsch ester, a hydrogen donor only, in place of amine resulted in a single turnover (Table S9), and iii) photoreduction using the cationic analog 2-H+ was successful, yet with lower yield (42% vs 83%, Figure 4b). These observations, along with our previous report on helicenium forming a helicene radical as a result of PET,[25] suggests a possible mechanism similar to the one reported by Nicewicz et. al. (Figure 4c).[22] Upon irradiation, the photoexcited radical 2-H•* undergoes single electron transfer (SET) to reduce the aryl halide, generating the cation 2-H+, aryl radical and halide anion. Then, photoexcitation of 2-H+ forms the excited state 2-H+*, which is reduced by DIPEA to regenerate the PC 2-H•. Meanwhile, DIPEA also serves as a hydrogen atom donor to convert the aryl radical intermediate to the corresponding arene.

Conclusion

In summary, we synthesized and isolated a series of [4]helicene quinacridyl radicals *2•–5•.* The spectroscopic, computational, and chemical characterization suggests that the nature of bridging group (N*R)* has little to no impact on the electronic structure, reactivity, and physical properties of these radicals, supporting that the unpaired spin resides predominantly in the heterocyclic π-system. Introduction of an

electron withdrawing group, *2-NO2•,* resulted in an enhanced stability, demonstrated by its SOMO energy, a less reducing E1/2 potential, and a longer lifetime when exposed to air. However, EPR spectroscopy and DFT calculations show that the electronic structure is virtually unaffected, suggesting that the unpaired electron in *2•–5•* is predominantly localized on the central carbon. Importantly, these radicals undergo a clean reversible oxidation upon exposure to air, as supported by UV-Vis spectroscopy. The same radical–cation reversibility can be observed electrochemically. Cyclic voltammograms of *2+–5+* indicated a highly reversible one-electron redox event for this process. Finally, the PET properties of *2-H•* were studied, producing moderate to high yields in the photoreduction of aryl halides, including a relatively unreactive aryl chloride, which represents the first isolated organic radical photocatalyst. Due to their high persistence, wide-range absorbance, and reversible redox properties, these helical radicals have great potential as photo-active molecules. Further investigation into the photocatalytic properties of these radicals is underway in our laboratory.

Declarations

We are grateful for financial support from the University of Arizona for this work. We thank Professor Rebecca Page and Dr. Michael Clarkson from the University of Arizona for Single crystal X-ray diffractions data collection. We thank Professors Elisa Tomat and Jon Njardarson from the University of Arizona, and Prof. Robert G. Bergman from UC Berkeley for helpful discussions.

References

1. Gomberg, M. An instance of trivalent carbon: tripehnylmethyl. *Am. Chem. Soc*. **22**, 757–771 (1900).
2. Buchachenko, A., Turton, C. & Turton, T. *Stable radicals*. (New York: Consultants Bureau 1965).
3. Kubo, T. Synthesis, physical properties, and reactivity of stable, π-conjugated, carbon-centered *Molecules* **24**, 665 (2019).
4. Hicks, R. G. Stable Radicals: Fundamental and Applied Aspects of Odd-electron Compounds. (Wiley-Blackwell: New York, 1–606, 2010).
5. Hicks, R. G. What's new in stable radical chemistry? *Biomol. Chem*. **5**, 1321 (2007).
6. Moad, G., Rizzardo, E. & Thang, S. H. Radical addition-fragmentation chemistry in polymer *Polymer* **49**, 1079–1131 (2008).
7. Kato, K., & Osuka, A. Platforms for stable carbon-centered radicals. *Chem., Int. Ed*. **58**, 8978- 8986 (2019).
8. Ingold, K. U. & Pratt, D. A. Advances in Radical-Trapping Antioxidant Chemistry in the 21st Century: A Kinetics and Mechanisms Perspective. *Rev*. **114**, 9022–9046 (2014).
9. Muldoon, M. J. et al. Aerobic oxidation catalysis with stable radicals. *Commun*. **50**, 4524–4543 (2014).
10. Matyjaszewski, K. & Xia, J. Atom Transfer Radical Polymerization. *Rev*. **101**, 2921–2990 (2001).

11. Ai, X. *et al.* Efficient radical-based light-emitting diodes with doublet emission. *Nature* **563**, 536–540 (2018).
12. Peng, Q., Obolda, A., Zhang, M. & Li, F. Organic light-emitting diodes using a neutral π radical as emitter: the emission from a doublet. *Chem., Int. Ed.* **54**, 7091–7095 (2015).
13. Obolda, A., Ai, X., Zhang, M. & Li, F. Up to 100% formation ratio of doublet exciton in deep-red organic light-emitting diodes based on neutral π-radical. *ACS Appl. Mater. Interfaces* **8**, 35472–35478 (2016).
14. Kumar, S., Kumar, Y., Keshri, S. K. & Mukhopadhyay, P. Recent advances in organic radicals and their magnetism. *Magnetochemistry* **2**, 42 (2016).
15. Ratera, I. & Veciana, J. Playing with organic radicals as building blocks for functional molecular materials. *Chem. Soc. Rev.* **41**, 303-349 (2012).
16. Sugawara, T., Komatsua, H. & Suzuki, K. Interplay between magnetism and conductivity derived from spin-polarized donor radicals. *Soc. Rev.* **40**, 3105-3118 (2011).
17. Rawson, J. M.; Alberola, A.; Whalley, A. Thiazyl radicals: old materials for new molecular devices. *Mater. Chem.* **16**, 2560-2575 (2006).
18. Romero, N. A. & Nicewicz, D. A. Organic Photoredox Catalysis. *Rev.* **116**, 10075–10166 (2016).
19. Koike, T. & Akita, M. Visible-light radical reaction designed by Ru- and Ir-based photoredox *Inorg. Chem. Front.* **1**, 562-576 (2014).
20. Yoshimi, Y. et al. Photoinduced electron transfer-promoted reactions using exciplex-type organic photoredox catalyst directly linking donor and acceptor arenes. *Molecules* **24**, 4453 (2019).
21. Ghosh, , Ghosh, T., Bardagi, J. I. & König, B. Reduction of aryl halides by consecutive visible light-induced electron transfer processes. *Science* **346**, 725–728 (2014).
22. Nicewicz, A. et al. Discovery and characterization of an acridine radical photoreductant. *Nature* **580**, 76– 80 (2020).
23. Scaiano, J. C., Tanner, M. & Weir, D. Exploratory Study of the Intermolecular Reactivity of Excited Diphenylmethyl Radicals. *Am. Chem. Soc.* **107**, 4396–4403 (1985).
24. Chow, Y. L., Buono-Core, G. E., Lee, C. W. B. & Scaiano, J. C. Sensitized Photoreduction of Bis(acetylacetonato)nickel(II) by Triplet State Aromatic *J. Am. Chem. Soc.* **108**, 7620–7627 (1986).
25. Mei, L., Veleta, J. M. & Gianetti, T. L. Helical carbenium: a versatile organic photoredox catalyst in red-light-mediated reactions. *Preprint.* DOI:10.26434/chemrxiv.12316154 (2020).
26. Rajca, A. et al. Radical cation and neutral radical of aza-thia[7]helicene with SOMO–HOMO energy level inversion. *Am. Chem. Soc.* **138**, 7298–7304 (2016).
27. Juríček, et al. Cethrene: a helically chiral biradicaloid isomer of heptazethrene. *Angew. Chem. Int. Ed.* **55**, 1183–1186 (2016).
28. Rajca, A. et al. Radical cation of helical, cross-conjugated β-oligothiophene. *Am. Chem. Soc.* **132**, 3246–3247 (2010).
29. Kato, , Furukawa, K., Mori, T. & Osuka, A. Porphyrin-based air-stable helical radicals. *Chem. - Eur. J.* **24**, 572–575 (2018).

30. Neunhoffer, O. & Haase, H. Dioxa-dihydrocoranthryl, a leveled triphenylmethyl radical. *Ber*. **91**, 1801(1958).
31. Neugebauer, A., Hellwinkel, D. & Aulmich, G. E.S.R. study of 12,12c-dihydro-4,4,8,8,12,12-hexamethyl-4H,8H-dibenzo[cd,mn]pyren-12C-yl, a planar triphenylmethyl. *Tetrahedron Lett*. **19**, 4871–4874 (1978).
32. Sørensen, T. J.; Nielsen, M. F. & Laursen, B. W. Synthesis and stability of N,N'-dialkyl-1,13-dimethoxyquinacridinium (DMQA+): a [4]helicene with multiple redox states. *ChemPlusChem 79*, 1030– 1035 (2014).
33. Ueda, et al. Chiral stable phenalenyl radical: synthesis, electronic-spin structure, and optical properties of [4]helicene-structured diazaphenalenyl. *Angew. Chem. Int. Ed*. **51**, 6691 –6695 (2012).
34. Martinm J. C. & Smith, R. G. Factors Influencing the Basicities of Triarylcarbinols. The Synthesis of Sesquixanthydrol. *Am. Chem. Soc*. **86**, 2252–2256 (1964).
35. Font-Sanchis, E., Aliaga, C., Focsaneanu, K.-S. & Scaiano, J. C. Greatly attenuated reactivity of nitrile-derived carbon-centered radicals toward oxygen. *Commun*. **2002**, 1576–1577 (2002).
36. Leehnig, M. et al. Sterically hindered free radicals. Part 22. Dimerization and EPR spectroscopy of indanedionyl and 9-acylf luorenyl radicals. *Chem. Soc. Perkin Trans.* **1**, 1247–1252 (1994).
37. Hartzler, H. D. Polycyano Radicals. *Org. Chem.* **31**, 2654–2658 (1966).
38. Bejan, E. V., Font-Sanchis, E. & Scaiano, J. C. Lactone-derived carbon-centered radicals: formation and reactivity with oxygen. *Org. Lett*. **3**, 4059–4062 (2001).

Figures

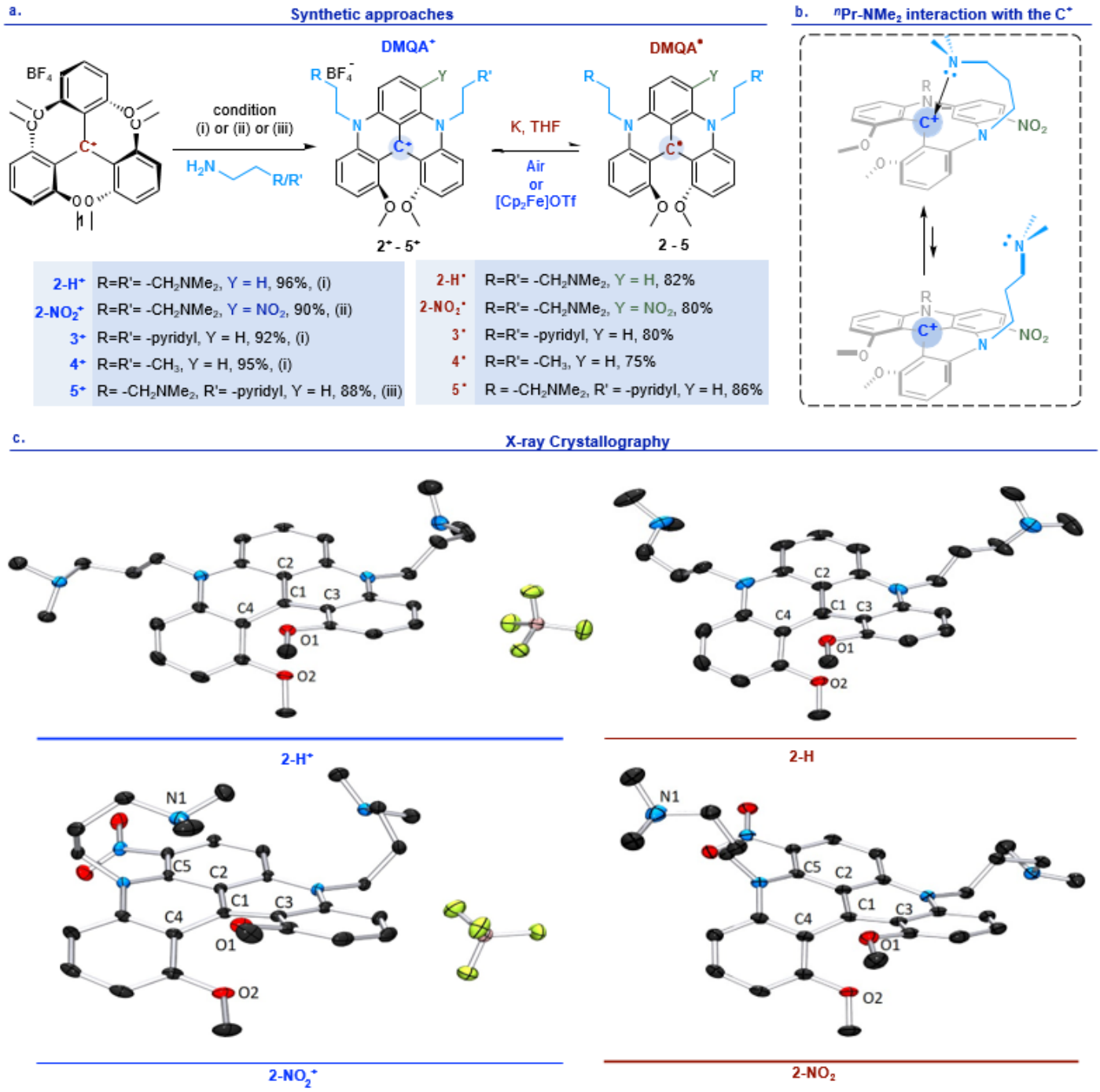

Figure 1

a. Synthetic schemes for cations and radicals: Synthesis of cations, (i) Synthetic route for 2-H+, 3+ and 4+: 1.0 equiv. of (1), 25.0 equiv of amine, CH3CN, 85 °C, 12 h; (ii) Synthetic route for 2-NO2+: 1.0 equiv. of (2+), HNO3 (67w%), 30 min; (iii) Synthetic route for 5+: 1.0 equiv. of (1), 1.2 equiv of 2-(2-Dimethylaminoethyl)pyridine, EtOAc, rt, 1.5 h; followed by 15.0 equiv of 3-(Dimethylamino)-1-propylamine, CH3CN, 85 °C, 12 h. Synthetic route for radicals, 2•−5•: 1.0 equiv. of (2+ - 5+), 1.1 equiv. of K or KC8 in THF, rt, overnight. b. Reversible interaction of the pendant amino group in the nPr-NMe2 bridge the

carbenium ion center suggested by NMR spectroscopy. c. X- ray structures of 2-H+, 2-H•, 2-NO2+, and 2-NO2•. Hydrogen atoms and solvent molecules are omitted for clarity.

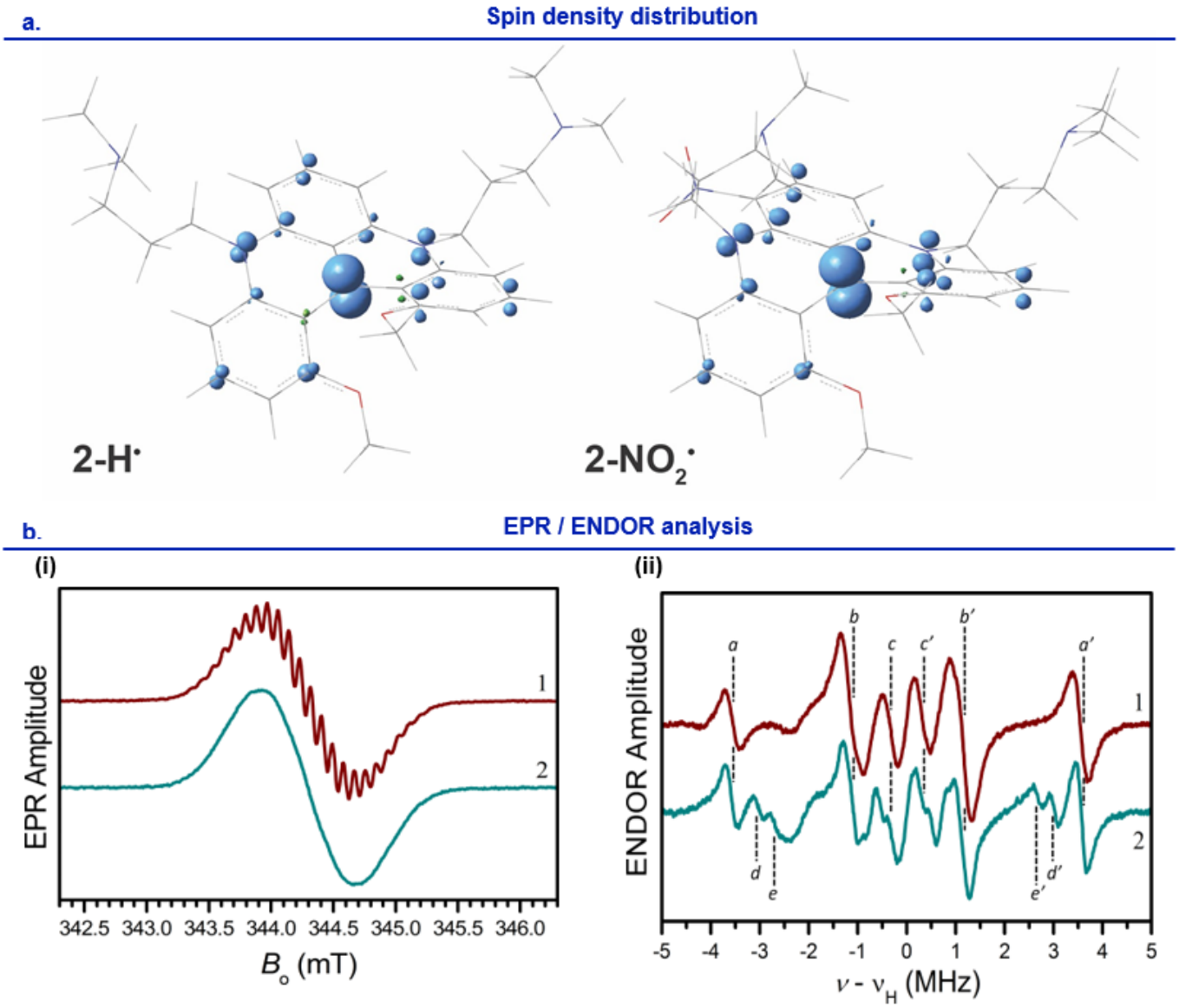

Figure 2

DFT calcluation and EPR/ENDOR spectroscopy. a, Spin density distribution for the calculated open- shell doublet models of 2-H• (left) and 2-NO • (right). Surfaces were plotted at a 0.015 isovalue. b, (i) CW EPR spectra of radicals 2-H• (trace 1) and 2-NO • (trace 2) in liquid toluene solutions at room temperature. Experimental conditions: mw frequency, 9.651 GHz; mw power, 2 mW; magnetic field modulation amplitude, 0.01 mT. (ii) CW ENDOR spectra of radicals 2-H• (trace 1) and 2-NO2• (trace 2) in liquid toluene-d8 solutions. Experimental conditions: mw frequency, 9.558 GHz; mw power, 32 mW; magnetic field, 340.9 mT (center of the EPR spectrum); radiofrequency (rf) power, 200 W; rf modulation amplitude, 100 kHz (frequency modulation); temperature, 210 K. The hfi constants estimated for each pair of ENDOR lines are: |aHa| ≈ 7.1 MHz (for a,a’ lines), |aHb| ≈ 2.3 MHz (for b,b’ lines), |aHc| ≈ 0.65 MHz (for c,c’ lines), |aHd| ≈ 6.1 MHz (for d,d’ lines), and |aHe| ≈ 5.4 MHz (for e,e’ lines).

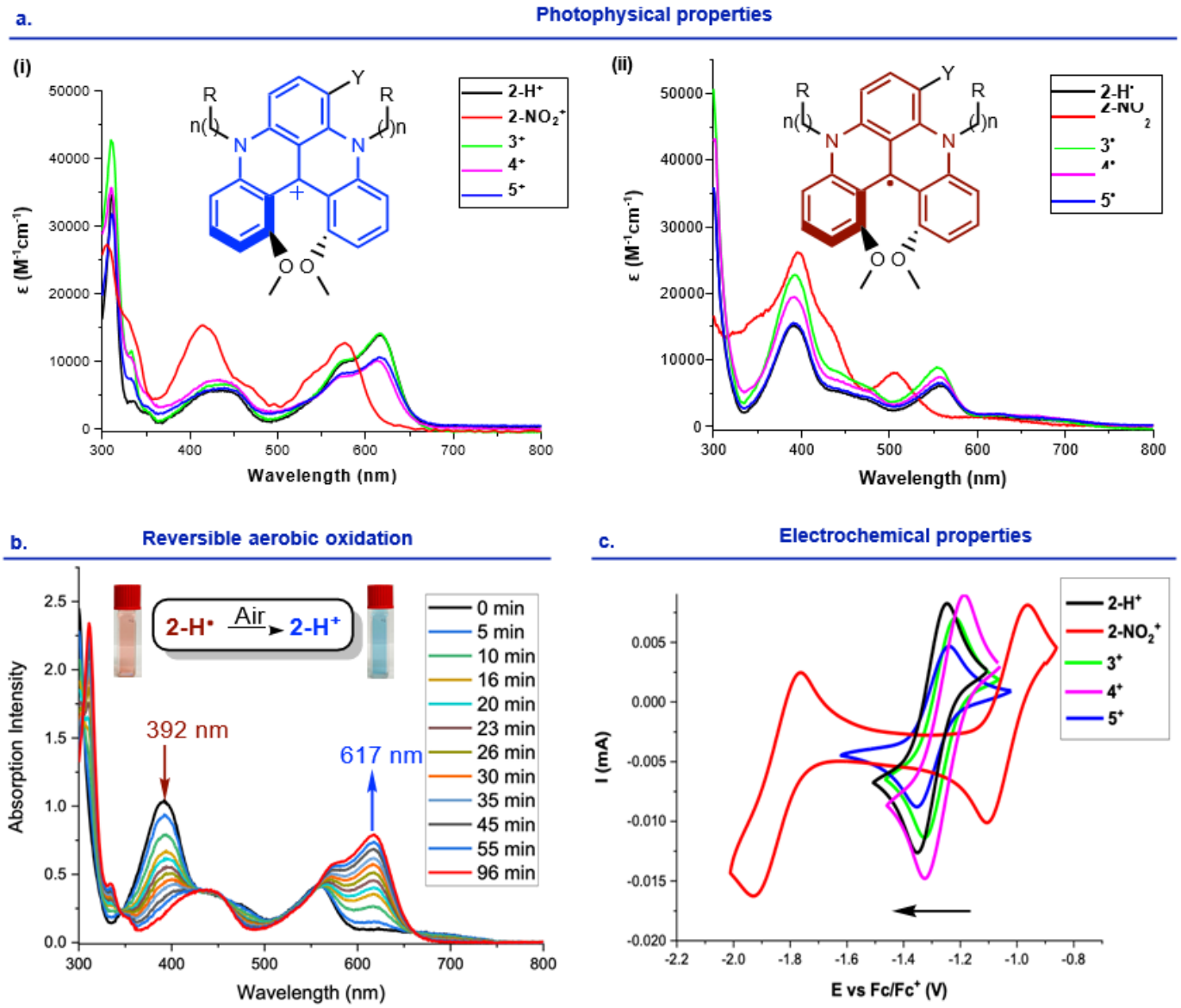

Figure 3

Electrochemical and spectroscopic analyses. a, UV-Vis spectroscopy; (i) Spectrum of heliceniums DMQA+ in PhCF3 (2+–5+), (ii) Spectrum of helicene radicals DMQA• in PhCF3 (2•–5•). b. Change of UV-visible absorption spectra of 2• in PhCF3 upon exposure to air. c. Cyclic voltammograms of 2+–5+ (2 mM) in DCM ([TBA][PF6] 0.1 M) solutions recorded at a platinum working electrode (v = 0.1 V/s) and Ag/Ag+ as internal reference electrode, Fc/Fc+ was used as secondary reference by setting its E1/2 = 0. The arrows indicate the direction of the scan. Reduction half-wave potential values (in V) measured by CV for 2-H+ (E red1 = -1.31), 2-NO + (E red1 = - 1.05, E red2 = -1.85), 3+ (E red1 = -1.26), 4+ (E red1 = -1.27), and 5+ (E red1 = -1.29), E versus the Fc/Fc+ redox couple.

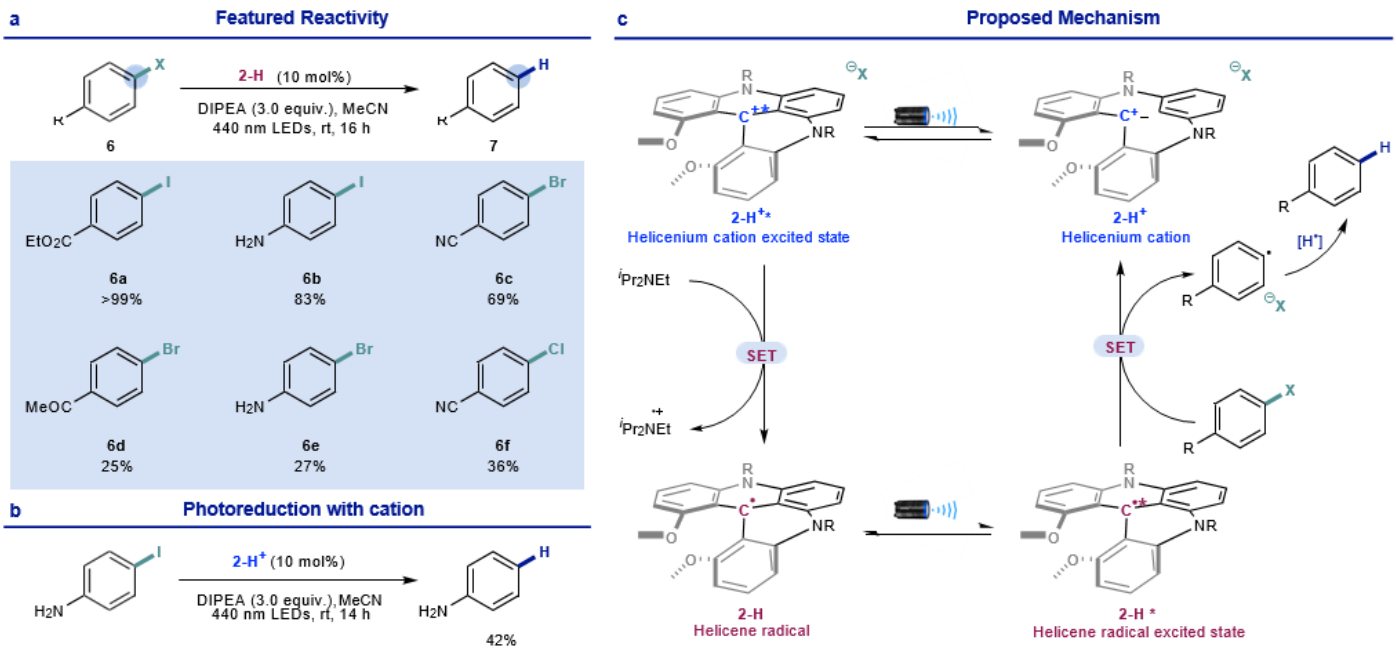

Figure 4

Photoreduction of aryl halides. a, Reaction scope with a helicene radical as photoredox catalyst. b, Photoreduction by helicenium cation. c, Proposed mechanistic pathway.

Supplementary Files

This is a list of supplementary files associated with this preprint. Click to download.

- GianettiRadicalESI.pdf